

# Decomposition of carbon dioxide to carbon by hydrogen-reduced Ni(II)-bearing ferrite

H. KATO, T. KODAMA, M. TSUJI, Y. TAMAURA\*

*Department of Chemistry, Research Center for Carbon Recycling and Utilization, Tokyo Institute of Technology, 2-12-1, Ookayama, Meguro-ku, Tokyo 152, Japan*

S. G. CHANG

*University of California, Lawrence Berkeley Laboratory, 1 Cyclotron Road, Berkeley, CA 94720, USA*

Hydrogen-activated Ni(II)-bearing ferrite,  $\text{Ni}_{0.37}^{2+}\text{Fe}_{0.49}^{2+}\text{Fe}_{2.09}^{3+}\text{O}_{4.00}$ , showed a high rate of decomposition of carbon dioxide to carbon at 300 °C. This is based on the redox process of the Ni(II)-bearing ferrite with the spinel type of crystal structure. The rates of both activation by hydrogen gas and oxidation in carbon dioxide gas were much improved in the Ni(II)-bearing ferrite. The rate of decomposition was  $0.178 \text{ mol h}^{-1}$  for the activated Ni(II)-bearing ferrite and  $0.00592 \text{ mol h}^{-1}$  for the activated magnetite in the batch mode, being 30 times larger. The rate of carbon dioxide decomposition was 16 times higher in the flow system in comparison with that of the activated magnetite.

## 1. Introduction

The decomposition and/or conversion of carbon dioxide ( $\text{CO}_2$ ) to carbon monoxide (CO) or hydrocarbon have been mostly studied using catalytic processes. The selectivity is relatively low even though these can be allowed to proceed at high temperatures of 600–800 °C. This requires a larger amount of energy than after reducing the  $\text{CO}_2$  level to atmospheric levels. One of the most effective solutions is the *in situ* decomposition of  $\text{CO}_2$  to carbon in each stationary source, e.g. power plant, steel plant, etc. The decomposition of the  $\text{CO}_2$  molecule to carbon has been reported to take place on the surface of the iron catalyst used in the Bosch reaction in the presence of hydrogen gas at 527–627 °C [1]. In this reaction, metallic iron is believed to play a central part in the decomposition of  $\text{CO}_2$  to carbon, but with hydrogen gas at 426–726 °C, the efficiency of  $\text{CO}_2$  decomposition to other compounds remained at 10%–20% at most [2, 3]. There have been no reports on the complete decomposition of  $\text{CO}_2$  with an efficiency of 100% at lower temperatures, which is desirable from the view point of energy saving and a reduction of the rate of  $\text{CO}_2$  emission to the atmosphere.

Recently, we have reported that the magnetite “activated” by hydrogen gas can decompose  $\text{CO}_2$  gas to carbon with a high selectivity of nearly 100% at a temperature as low as 290 °C [4].  $\text{CO}_2$  decomposition on the magnetite is a specific adsorption and is based on the redox process, coupled with a breaking reaction of  $\text{CO}_2$  to carbon on the activated magnetite  $\text{Fe}_3\text{O}_{4-\delta}$ . The process can be considered in terms of a

three-part model of adsorption and is briefly described as follows [5]. The oxygens of the adsorbed  $\text{CO}_2$  molecule are incorporated into the oxygen-deficient site of the activated magnetite to form elementary carbon, where the spinel-type structure is retained.

Ferrites belong to the same spinel group of crystals. They were used for the study of the effect of substitution of divalent transition metals in magnetite on their reactivity for the decomposition of  $\text{CO}_2$ . Mn(II) ferrite showed a non-specific adsorption [6]. The amount of evolved carbon increased with decrease in the content of manganese, attaining a maximum at the mole ratio of Mn/Fe = 0.1 [7]. Active wüstite prepared from Zn(II)-bearing ferrite with the chemical composition of  $\text{Zn}_{0.95}\text{Fe}_{2.04}\text{O}_{4.00}$  was reported to show  $\text{CO}_2$  decomposition to CO and carbon at 300 °C [8]. In these reactions, no metal carbides have been observed [8, 9].

The present paper describes the reactivity of the decomposition of  $\text{CO}_2$  to carbon on hydrogen-activated Ni(II)-bearing ferrite.

## 2. Experimental procedure

### 2.1. Synthesis of Ni(II)-bearing ferrite and magnetite

Ni(II)-bearing ferrite and magnetite were synthesized by air oxidation of a hydroxide suspension of Fe(II) with or without nickel sulphate, according to the wet method reported previously [10–13]. Requisite portions of  $\text{FeSO}_4 \cdot 7\text{H}_2\text{O}$  (typically 312 g) and  $\text{NiSO}_4 \cdot 6\text{H}_2\text{O}$  were dissolved in oxygen- and  $\text{CO}_2$ -free

\* Author to whom all correspondence should be addressed.

distilled water prepared by passing nitrogen gas through them for a few hours. The pH of the solution was adjusted to 10 by adding  $3.0 \text{ mol dm}^{-3}$  NaOH solution to form hydroxide suspension. Air was passed through the alkaline suspension for oxidation for 24 h at  $65^\circ\text{C}$ , while the pH was kept constant at 10 by adding the  $3.0 \text{ mol dm}^{-3}$  NaOH solution. The product was collected by decantation. After washing with acetate buffer solution, distilled water, and acetone successively, the product was dried in a nitrogen stream at ambient temperature. The product was characterized by X-ray diffractometry (XRD) with  $\text{CuK}_\alpha$  radiation (Rigaku, RINT 1100 diffractometer) and Mössbauer spectroscopy. All the Mössbauer spectra were recorded at room temperature with a  $^{57}\text{Co}$  source diffused in metallic rhodium which was oscillated in a constant acceleration mode. The spectra were calibrated with a thin absorber of an  $\alpha\text{-Fe}$  foil. The source was supplied by NEN (UK). The chemical compositions of the products were determined by atomic absorption spectroscopy for the total contents of nickel and iron, and by colorimetry (Hitachi spectrophotometer, model 124) using 2, 2' dipyridyl for identification of Fe(II) and Fe(III). Ni(II)-bearing ferrite was determined for metallic content after Ni(II) and Fe(II) were separated from Fe(III) using a Dowex 1X8 anion exchange resin column (1 cm inner diameter  $\times$  12 cm long) [14].

## 2.2. Activation of magnetite and ferrites

The conditions for the activation of magnetite and ferrite were studied using a thermogravimeter (Shimadzu TGA-50). Ni(II)-bearing ferrite or magnetite was taken in a small quartz cell of 5 mm inner diameter  $\times$  2.7 mm deep. Hydrogen gas was passed through at a flow rate of  $50 \text{ cm}^3 \text{ min}^{-1}$  at  $300^\circ\text{C}$  to study the activation of the materials. The formed activated ferrite was allowed to react in a flow of  $\text{CO}_2$  gas at  $300^\circ\text{C}$ .

## 2.3. Decomposition of $\text{CO}_2$

The decomposition of  $\text{CO}_2$  with the hydrogen-reduced Ni(II)-bearing ferrite and magnetite was studied using a reaction cell in the batch system in a similar way to that reported previously [6]. Ni(II)-bearing ferrite or magnetite (3.0 g) was placed in a quartz tube (reaction cell 2 cm inner diameter  $\times$  20 cm long), evacuated and heated to  $300^\circ\text{C}$  in an electric furnace. The hydrogen-reduced magnetite and Ni(II)-bearing ferrite were prepared by passing hydrogen gas at a flow rate of  $50 \text{ cm}^3 \text{ min}^{-1}$  through magnetite and Ni(II)-bearing ferrite powder for 1.5 h at  $300^\circ\text{C}$ . A given volume of  $\text{CO}_2$  gas was injected into the reaction cell using a gas-tight syringe. The inner gas species were determined as a function of time by gas chromatography using gas chromatography equipment, Shimadzu model GC-8A. The sample was quenched by placing the reaction cell into a refrigerant of ice/NaCl while passing nitrogen gas through the reaction cell for XRD, and then removed in a nitrogen atmosphere while protecting it from oxidation. De-

posited carbon was collected by filtering with quartz wool after dissolving the samples in HCl solution, and determined using an elemental analyser (Perkin-Elmer, model 2400 CHN).

## 3. Results and discussion

### 3.1. Ni(II)-bearing ferrite and magnetite

X-ray diffraction patterns (XRD) of these materials confirmed that these products consisted of a single phase of the spinel-type compound without any other peaks due to  $\alpha\text{-Fe}_2\text{O}_3$  and iron oxide hydroxides such as  $\alpha\text{-FeO(OH)}$ . The lattice parameters,  $a_0$ , were  $0.83870(4) \text{ nm}$  for Ni(II)-bearing ferrite and  $0.8390 \text{ nm}$  for magnetite. The chemical composition of magnetite was determined to be  $\text{Fe}_{2.91}\text{O}_4$  which shows deviation from the stoichiometric composition. Hence, the synthesized magnetite was slightly oxidized and expressed as the solid solution of  $0.67(\text{Fe}_3\text{O}_4) - 0.33(\gamma - \text{Fe}_2\text{O}_3)$  for the chemical composition [15]. The chemical composition of Ni(II)-ferrite was  $\text{Ni}_{0.37}^{2+}\text{Fe}_{0.49}^{2+}\text{Fe}_{2.09}^{3+}\text{O}_{4.00}$ . The mole ratio of Ni/Fe was in good agreement with that of the starting reaction suspensions, indicating that  $\text{Ni}^{2+}$  was quantitatively incorporated into the spinel-type of ferrite in the air-oxidation of Fe(II) hydroxide suspension.

In the infrared spectrum of the Ni(II)-bearing ferrite, absorption bands appeared at  $590$  and  $360 \text{ cm}^{-1}$  characteristic of ferrite. The former band is due to vibration of the bond of metal to the tetrahedral oxygen, and the latter is assigned to the vibration of the oxygen in a direction almost perpendicular to the former vibrations [16]. The infrared spectrum showed that the products contained no amorphous by-products of Fe(III) oxide hydroxides, such as  $\alpha\text{-FeO(OH)}_3$ , and  $\text{Ni(OH)}_2$ ; the absorption bands at  $800\text{--}1100 \text{ cm}^{-1}$ , characteristic of the Fe(III) oxide hydroxides such as  $\alpha$ -,  $\beta$ -,  $\delta$ -, and  $\gamma\text{-FeO(OH)}$ , and  $\text{Ni(OH)}_2$  [17], were not observed. From these results, almost all of the Ni(II) ions in the product are considered to be incorporated into the ferrite.

The prepared magnetite gave the expected Mössbauer spectrum consisting of two sextets of I and II (Fig. 1a). Sextet I is due to  $\text{Fe}^{3+}$  in the tetrahedral (A) and octahedral (B) sites, and sextet II is due to the paired ions of  $\text{Fe}^{2+}$  and  $\text{Fe}^{3+}$  in the octahedral (B) sites ( $\text{Fe}^{2.5+}$ ) in the spinel structure [7, 18]. The proportion of areas I and II was equal, and also in good agreement with that calculated: 51% for sextet I, and 49% for sextet II, based on the chemical composition assuming that the vacancies and  $\text{Fe}^{2+}$  occupy the B sites, and that  $\text{Fe}^{3+}$  is distributed in both A and B sites. Fig. 1b shows the Mössbauer spectrum of Ni(II)-bearing ferrite. Magnetically split patterns with two sextets appeared, but sextet II was broadened in comparison with that of the magnetite. Such broadening has not been reported for Mössbauer spectra of  $\text{Fe}_3\text{O}_4$  nor the solid solution of  $\text{Fe}_3\text{O}_4$  and  $\gamma\text{-Fe}_2\text{O}_3$  [19]. It can be considered that the broadening was caused by the incorporation of Ni(II) ions into the spinel structure of the ferrite. The broadening of pattern II shows that the electron hopping between  $\text{Fe}^{2+}$  and  $\text{Fe}^{3+}$  is not fast enough to restore the natural peak width.

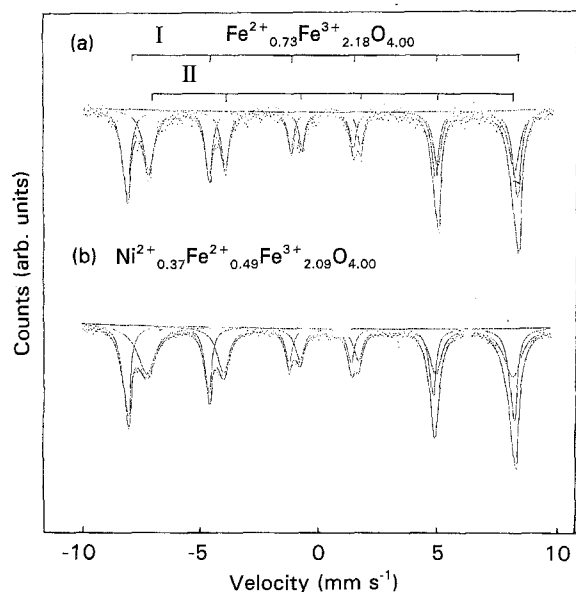


Figure 1 Mössbauer spectra of (a) magnetite and (b) Ni(II)-bearing ferrite.

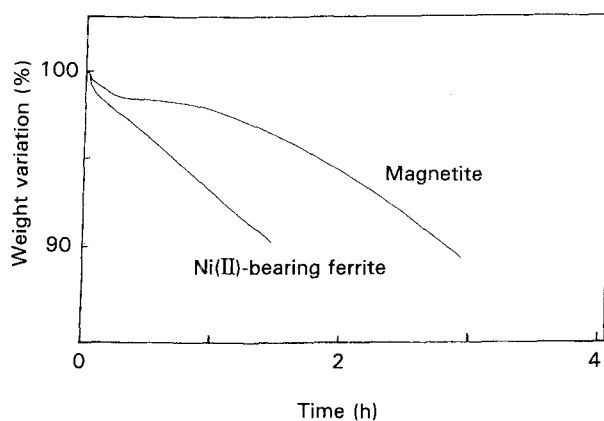


Figure 2 Rate of reduction of magnetite and Ni(II)-bearing ferrite in a flow of hydrogen gas at 300 °C.

Robbins *et al.* [20] pointed out that such broadening was also observed in a chromium ferrite. This indicates that  $\text{Ni}^{2+}$  was incorporated into the lattice sites in the spinel structure of the ferrite.

### 3.2. Reduction and oxidation curve

The reduction process of magnetite in a flow of hydrogen gas was facilitated by Rh(III)-impregnation in magnetite [21]. The rate and temperature of reduction are very important in predicting the reactivity for decomposition of  $\text{CO}_2$  to CO and/or carbon. The initiation temperature of reduction, i.e. activation, of magnetite (354 °C) was lowered to 282 °C, the extent of this lowering being independent of the amount of loaded Rh(III) and large in comparison with a physical mixture of magnetite and metallic rhodium. The Rh(III)-bearing magnetite was reduced rapidly in a flow of hydrogen gas at 250 °C, and the rate of reduction was approximately 350 times higher than that of magnetite. In the present research, magnetite was rapidly reduced in the initial stage of reaction with

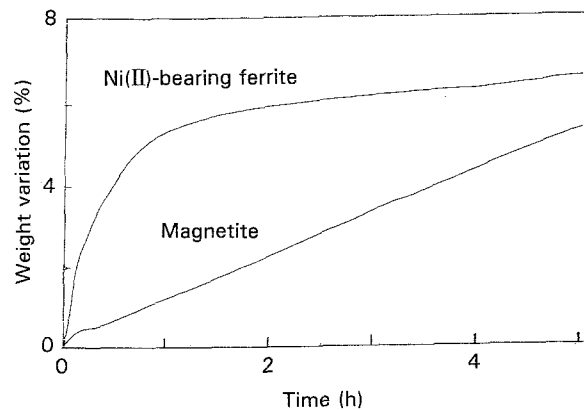


Figure 3 Rate of oxidation of hydrogen-activated magnetite and Ni(II)-bearing ferrite in a flow of  $\text{CO}_2$  gas at 300 °C.

hydrogen gas and then the reduction proceeded gradually through a small steady state of reaction on the thermogravimetric curve at 300 °C (Fig. 2). The rapid decrease in the initial stage of the process will involve the transformation of the  $\gamma\text{-Fe}_2\text{O}_3$  component to  $\text{Fe}_3\text{O}_4$  phase. The prolonged reduction by hydrogen gas produced a small metallic iron which will be reactive with respect to  $\text{CO}_2$  reduction. Ni(II)-bearing ferrite was much more rapidly reduced than magnetite, suggesting outstanding reactivity for  $\text{CO}_2$  decomposition. It was reduced linearly with respect to time. The reduced materials were oxidized in a flow of  $\text{CO}_2$  gas at 300 °C (Fig. 3). Magnetite was linearly oxidized and Ni(II)-bearing ferrite was rapidly oxidized within 1 h. These profiles show a high rate of redox process at 300 °C.

### 3.3. Decomposition of $\text{CO}_2$ with hydrogen-reduced Ni(II)-bearing ferrite and magnetite

Fig. 4 shows the rate of  $\text{CO}_2$  decomposition over hydrogen-reduced magnetite and Ni(II)-bearing ferrite at 300 °C. The hydrogen-reduction was carried out while the spinel structure was retained. No evidence of metallic nickel was observed in the XRD pattern of the hydrogen-reduced Ni(II)-bearing ferrite. The  $\text{CO}_2$  content gradually decreased with reaction time on magnetite, and  $\text{CO}_2$  in the reaction cell diminished to 27% after 40 min. However, for the hydrogen-reduced Ni(II)-bearing ferrite, the  $\text{CO}_2$  content decreased with reaction time at a higher rate than that for the hydrogen-reduced magnetite, and about 99% of the  $\text{CO}_2$  diminished in 40 min. The hydrogen-reduced Ni(II)-bearing ferrite has a higher reactivity for the  $\text{CO}_2$  decomposition than that of hydrogen-reduced magnetite. The rate of oxidation in the initial stage was 16 wt %  $\text{h}^{-1}$  for Ni(II)-bearing ferrite and 1.0 wt %  $\text{h}^{-1}$  for magnetite. The decomposition rate of  $\text{CO}_2$  was 0.178 mol  $\text{h}^{-1}$  for Ni(II)-bearing ferrite and 0.00592 mol  $\text{h}^{-1}$  for magnetite. The reactivity of the former material was 16 times larger in the continuous mode of  $\text{CO}_2$  decomposition and 30 times larger in the batch mode of  $\text{CO}_2$  decomposition. Thus, the rate of the decomposition of  $\text{CO}_2$  to carbon was substantially

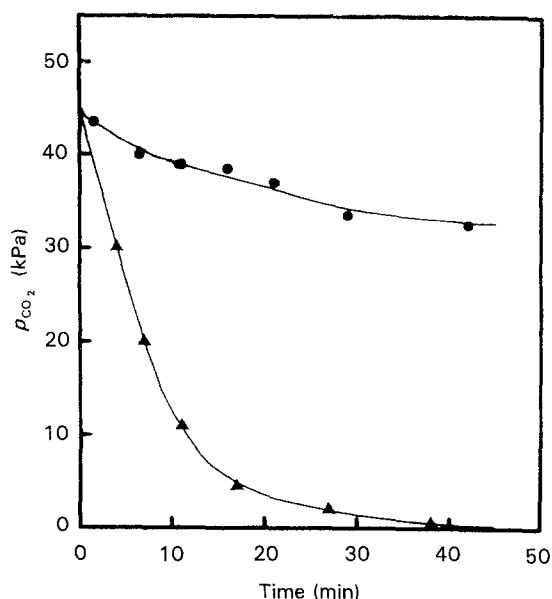


Figure 4 Change in  $p_{\text{CO}_2}$  as a function of time for reaction with (●) activated magnetite and (▲) Ni(II)-bearing ferrite at 300 °C. Material, 3.0 g; conditions for hydrogen-reduction: 1.5 h in a flow rate of 50 cm<sup>3</sup> min<sup>-1</sup>; amount of injected CO<sub>2</sub>, 10 cm<sup>3</sup>.

improved: approximately one order in the decomposition rate in comparison with the hydrogen-reduced magnetite. The remarked reactivity toward the decomposition of CO<sub>2</sub> to carbon on the Ni(II)-bearing ferrite can be considered as follows. The reduced nickel formed on the surface is very active, facilitating both the degree of activation of Ni(II)-bearing ferrite through dissociation of the hydrogen molecule over reduced nickel, and the decomposition  $\text{CO}_2 \rightarrow \text{C} + 2\text{O}_{(\text{ad})}$ .

The hydrogen-reduced Ni(II)-bearing ferrite after the CO<sub>2</sub> decomposition was determined for the carbon powder collected by dissolving the sample in the HCl solution: it was only 51% of the diminished CO<sub>2</sub> by volume. The large difference can be ascribed to the following reasons. Two types of carbon have been reported to be deposited on the metallic nickel catalyst: dispersed ( $\alpha$ ) and polymerized ( $\beta$ ) forms [22]. The  $\alpha$  state carbon is considered to be isolated carbon atoms on the surface, and carbon in the  $\beta$  state is assigned to polymerized carbon. In the present work, at least two types of carbon were probably deposited on the surface. The atomic carbon could not be collected by the present procedure of dissolving sample in

the HCl solution, because the very small elementary carbon will be washed out.

### Acknowledgements

Part of this research was financially supported by a Grant-in-Aid for Science Research 03203216 from the Ministry of Education, Science and Culture. T. Kodama is grateful for grants from Fellowships of the Japan Society for the Promotion of Science for Japanese Junior Scientists.

### References

1. A. SACCO, Jr and R. C. REID, *Carbon* **17** (1979) 459.
2. R. C. WAGNER, R. CARRASQUILLO, J. EDWARDS and R. HOLMES, in "Proceedings of 18th Intersociety Conference on Environmental Systems", SAE Technical Paper Series 880995, Society of Automotive Engineers, Warrendale PA (1988).
3. M. LEE, J. LEE and C. CHANAG, *J. Chem. Eng. Jpn* **23** (1990) 130.
4. Y. TAMAURA and M. TABATA, *Nature* **346** (1990) 225.
5. K. NISHIZAWA, T. KODAMA, M. TABATA, T. YOSHIDA, M. TSUJI and Y. TAMAURA, *J. Chem. Soc. Farad. Trans.* **88** (1992) 2771.
6. M. TABATA, Y. NISHIDA, T. KODAMA, K. MIMORI, T. YOSHIDA and Y. TAMAURA, *J. Mater. Sci.* **28** (1993) 971.
7. M. TABATA, K. AKANUMA, K. NISHIZAWA, T. YOSHIDA, M. TSUJI and Y. TAMAURA, *ibid.* **28** (1993) 6753.
8. T. KODAMA, K. TOMINAGA, M. TABATA, T. YOSHIDA and Y. TAMAURA, *J. Amer. Ceram. Soc.* **75** (1992) 1287.
9. K. AKANUMA, M. TABATA, T. YOSHIDA, M. TSUJI and Y. TAMAURA, *J. Mater. Chem.*, **3** (1993) 943.
10. Y. TAMAURA, S. MECHAIMONCHIT and T. KATSURA, *J. Inorg. Nucl. Chem.* **43** (1980) 671.
11. T. KATSURA, Y. TAMAURA and G. S. CHYO, *Bull. Chem. Soc. Jpn* **52** (1979) 96.
12. Y. TAMAURA, P. V. BUDUAN and T. KATSURA, *J. Chem. Soc. Dalton Trans.* (1981) 1807.
13. M. KIYAMA, *Bull. Chem. Soc. Jpn* **47** (1974) 1646.
14. K. A. KRAUS and G. E. MOORE, *J. Am. Chem. Soc.* **75** (1953) 1460.
15. T. KODAMA, *J. Mater. Chem.* **2** (1992) 525.
16. R. D. WALDRON, *Phys. Rev.* **99** (1955) 1972.
17. T. MISAWA, K. HASHIMOTO and S. SHIMODAIRA, *Boshoku Gijutsu (Corros. Eng.)* **23** (1974) 17.
18. H. FRANKE and M. ROSENBERG, *J. Magn. Mag. Mater.* **9** (1979) 74.
19. K. VOLENÍK, M. SEBERÍNI and J. NEID, *Czech. J. Phys.* **B25** (1975) 1063.
20. M. ROBBINS, G. K. WERTHEIM, R. C. SHERWOOD and D. N. E. BUCHANAN, *J. Phys. Chem. Solids* **32** (1971) 717.
21. K. AKANUMA, K. NISHIZAWA, T. KODAMA, M. TABATA, K. MIMORI, T. YOSHIDA, M. TSUJI and Y. TAMAURA, *J. Mater. Sci.* **28** (1993) 860.
22. J. G. McCARTY and H. WISE, *J. Catal.* **57** (1979) 406.

Received 11 June 1993

and accepted 16 May 1994